Preprints of the 19th World Congress
The International Federation of Automatic Control
Cape Town, South Africa. August 24-29, 2014

Energy Management of Parallel Hybrid Electric Vehicles based on Stochastic Model Predictive Control ⋆

M. Joševski * **D. Abel** *

* *Institute of Automatic Control, Department of Mechanical Engineering, RWTH Aachen University, Germany, (e-mail: M.Josevska@irt.rwth-aachen.de, D.Abel@irt.rwth-aachen.de).*

Abstract: This paper proposes a control approach for the energy management of parallel hybrid electric vehicles based on stochastic model predictive control (SMPC). Apart from minimizing fuel consumption, the controller additionally accounts for CO_2 emissions. Considering the vehicle's velocity to be time-varying, the limits for both propulsion machines of the hybrid vehicle are determined over a multiple prediction horizon. The stochastic approach has the advantage that the future driving profile does not have to be known in advance but is predicted based on an underlying stochastic model of the driver behavior. Simulation results obtained on standard driving cycles such as NEDC demonstrate the potential of the SMPC approach compared to a MPC controller with a-priori knowledge of the driving cycle.

Keywords: energy management systems, hybrid vehicles, stochastic modeling, model based control, Markov models

1. INTRODUCTION

1.1 Motivation

Passenger vehicles are a major source of greenhouse gas emissions, producing around 15% of the EU's emissions of CO_2. While emissions from other sectors are generally decreasing, those from transport have considerably increased in the last decades. In addition to a European Commission strategy adopted in 2007, the EU has put in place a comprehensive legal framework to reduce CO_2 emissions of passenger vehicles. The legislation sets binding emission targets for automobile manufacturers that are obligated to ensure that new vehicles do not emit more than an average of 130g CO_2 per kilometer by 2015 and 95g by 2020. Apart from this long-term target the strategy sets limitations regarding fuel consumption. With the sources of oil being limited the caution measures have to be taken regarding their exploration and their negative environmental influence. One of the modalities to achieve the fuel consumption and gas emission reduction is to increase the share of alternative fuel vehicle technologies such as hybrid electric vehicles (HEVs) on the market. In addition to increasing the share of fuel efficient technologies, improvements in energy management strategies used in HEVs can contribute in reaching the set environmental protection goals.

HEVs use at least two different energy sources for their propulsion. Frequently an internal combustion engine (ICE) is combined with one or more electric machines (EM) and an energy buffer. This provides them additional degree of freedom that allows for more efficient operation. Compared to conventional vehicles, HEVs can significantly improve fuel economy due to their ability to recover the kinetic energy during braking and optimize the operation of the propulsion system.

⋆ This work was founded by the German Research Foundation (grant number AB-65/11-1).

1.2 Related Work and Main Contribution

In order to be able to achieve better fuel economy many control strategies have already been proposed for HEVs such as heuristic methods (HM) (see Guzzella and Sciaretta [2013]), deterministic dynamic programming (DP) (see Wang and Lukic [2012], Sundstrom and Guzzella [2009]), stochastic dynamic programming (SDP) (see Liu and Peng [2008], Tate et al. [2007], Johannesson et al. [2005], Opila et al. [2012]), equivalent consumption minimization strategy (ECMS) (see Serrao et al. [2009], Musardo et al. [2005]), model predictive control (MPC) (see Beck et al. [2005], Borhan et al. [2012]) and game theory (GT) (see Dextreit and Kolmanovsky [2013]). All of these approaches have the goal to minimize fuel consumption while keeping the propulsion system components within reasonable operating limits.

Heuristic or rule-based methods achieve good performance but only when designed for specific vehicle and specific driving conditions. Deterministic dynamic programming provides a global optimum for the power split between the internal combustion engine and the electric machine in terms of reduced fuel consumption. Unfortunately, the necessity of knowing the driving cycle in advance in order to solve the optimization problem and the high computational burden makes this nonlinear method inappropriate for real-time application. While dynamic programming uses a deterministically given driving cycle stochastic dynamic programming, as presented in Liu and Peng [2008],

Tate et al. [2007], Johannesson et al. [2005] and Opila et al. [2012], approximates the future driving profile by a stochastic process. In Ripaccioli et al. [2010], Bichi et al. [2010] and Di Cairano et al. [2013] a stochastic model predictive control algorithm (SMPC) was proposed as control strategy for HEVs and realized on the example of a series HEV. Combining the stochastic driving profile with the idea of receding horizon control enables the estimation of the future driver behavior for the whole prediction horizon.

In this publication a stochastic model predictive control strategy is proposed and the controller performance is evaluated on standard driving cycles. Compared to Ripaccioli et al. [2010], a parallel HEV model is used that is based on torques instead of power demands. Furthermore, the vehicle's velocity is considered to be time-varying over the prediction horizon. In this way, the actual machine limits in terms of minimum and maximum torques that depend on the rotational speed can explicitly be considered over the prediction horizon in the predictive control scheme. The future driver behavior is represented by a Markov chain with finite number of states. Thereby the driver torque demand has been selected as state of the Markov chain. Identifying a Markov chain requires the estimation of transition probabilities which are commonly determined based on a frequency analysis. In contrast to Ripaccioli et al. [2010] and Di Cairano et al. [2013], where ordinary maximum likelihood estimation is used, in this publication a smoothing technique, as described in section 3, is employed in order to conduct the learning process. In addition to previous publications, apart from the mass fuel rate, CO_2 emissions are considered in the optimization problem as well. This paper is organized as follows: in section 2 the considered HEV model employed for optimization is presented. Section 3 provides details on the employed stochastic model of the driver behavior. The formulation of a standard MPC scheme as well as the applied SMPC optimization problem are outlined in section 4. Finally simulation results and a comparative analysis of a MPC reference controller and the SMPC implementation is provided in section 5.

2. HYBRID VEHICLE MODEL

In the energy management strategy a parallel HEV architecture has been considered as depicted in Fig. 1. The engine and electric machine are mechanically linked to the wheels. The following torque balance relation describes the proposed coupling:

$$T_{wh}(t) = \eta_{gb} \cdot R(i(t)) \cdot (T_{em}(t) + T_{ice}(t)) + T_{br}(t) \quad (1)$$

where $T_{wh}(t)$ is the torque at the wheels, η_{gb} the transmission efficiency which is considered to be constant, $R(i(t))$ the transmission ratio depending on the gear $i(t)$ and $T_{em}(t)$, $T_{ice}(t)$, $T_{br}(t)$ are the torque of the electric machine, the engine torque and the conventional braking torque respectively.

The angular velocities of the combustion engine and the electric machine are defined as:

$$\omega_{ice}(t) = \omega_{em}(t) = \eta_{gb} \cdot R(i(t)) \cdot \omega_{wh}(t) \quad (2)$$

where $\omega_{wh}(t)$ denotes the rotational speed of the wheel. Both rotational speeds and torques are limited by mechanical constraints. The minimum and maximum torques are provided by maps for the engine and electric machine.

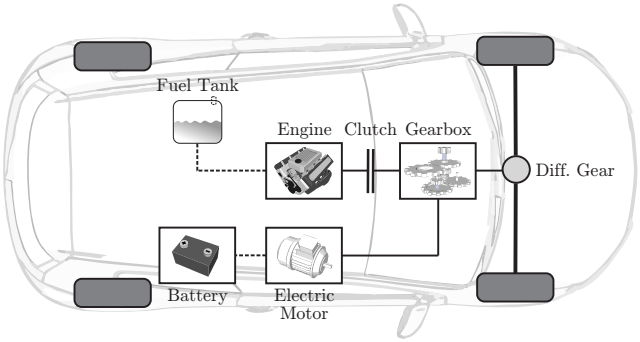

Fig. 1. Parallel hybrid electric vehicle configuration

2.1 Engine Model

In modeling of the internal combustion engine its dynamics are neglected as the time constant of the engine is significantly lower than controller sampling time T_s (here taken to be $T_s = 1\,\mathrm{s}$). In this context only the fuel consumption and gas emissions are considered. The fuel consumption is modeled by a nonlinear map which depends on the ICE torque T_{ice} and the rotational speed ω_{ice}:

$$\dot{m}_f(T_{ice}(t), \omega_{ice}(t)) = f_{\dot{m}_f}(T_{ice}(t), \omega_{ice}(t)) \quad (3)$$

This nonlinear relation is approximated by a polynomial of the form:

$$\dot{m}_f(T_{ice}(t), \omega_{ice}(t)) \approx \sum_{i=0}^{3} \sum_{j=0}^{3} a_{ij} \cdot \omega_{ice}^i \cdot T_{ice}^j \quad (4)$$

and used later in the optimization procedure to approximate the expression for the fuel consumption. The goal is to make the model as simple as possible while still being useful for the optimization algorithm. Apart from fuel consumption, CO_2 emissions are considered and minimized. In a similar way as fuel consumption the nonlinear function describing the CO_2 emissions is given by map of the form:

$$\dot{m}_{CO_2}(T_{ice}(t), \omega_{ice}(t)) = f_{CO_2}(T_{ice}(t), \omega_{ice}(t)) \quad (5)$$

Similar to (4) this relation has been approximated by a third order polynomial of the engine angular velocity ω_{ice} and torque T_{ice} and is applied in the control scheme described in section IV. The maximum torque of the engine is a function of its angular velocity:

$$T_{ice,max} = f_{ice,max}(\omega_{ice}) \quad (6)$$

2.2 Electric Machine Model

The electric machine is designed to be able to meet the higher torque demands. In addition to this the EM is also used to recuperate the braking energy up to the point when either its torque limit $T_{em,min}(\omega(t))$ or the battery charging limit has been reached, after which friction brakes are activated. Similarly to the engine model, the dynamic behavior is neglected and the electric machine is modeled by an efficiency map which is a nonlinear function of the torque T_{em} and the angular velocity ω_{em}:

$$\eta_{em}(T_{em}(t), \omega_{em}(t)) = f_{\eta_{em}}(T_{em}(t), \omega_{em}(t)) \quad (7)$$

Based on the efficiency map the power of electric machine is gained as:

$$P_{em}(t) = f_{em}(\eta_{em}(T_{em}(t), \omega_{em}(t)), \omega_{em}(t), T_{em}(t)) \quad (8)$$

However in the optimization model this relation has been approximated by a third order polynomial similar to (4).

The minimum and maximum torques $T_{em,min}(\omega_{em}(t))$ and $T_{em,max}(\omega_{em}(t))$ are given by a map in dependence of the EM rotational speed as:

$$T_{em,max} = f_{em,max}(\omega_{em}),\ T_{em,min} = -f_{em,max}(\omega_{em}) \quad (9)$$

In this publication no concrete hybrid vehicle has been considered. Thereby all the necessary quantitative values, efficiency maps for both machines as well as the fuel consumption and CO_2 emissions maps have been taken from ADVISOR simulation tool, see Wipke et al. [1999].

2.3 Battery Model

The state of charge (SoC) of the battery is the amount of electrical energy stored in it. The change of the SoC is described by:

$$\dot{SoC}(t) = -\frac{P_{batt}(t)}{Q_{max} \cdot U_{nom}} \quad (10)$$

where P_{batt} denotes the battery power, Q_{max} the nominal battery capacity and U_{nom} its nominal voltage. To ensure a prolonged life of the energy buffer, the battery state of charge should be kept close to a certain set-point and the battery should operate within a prescribed, allowed range. In this paper a range between 50% -70% is considered. Some effects have been neglected. Actually, the internal resistance and open circuit voltage depend on the state of charge. However for the sake of simplicity open circuit voltage is approximated by a constant voltage level and losses due to internal resistance are not considered.

2.4 Vehicle Model

The vehicle is modeled as a point mass and only longitudinal dynamics is considered:

$$T_{wh}(t) = r_{wh}(m_{veh} \cdot g \cdot \sin(\theta) + m_{veh} \cdot g \cdot f_r \cdot \cos(\theta) + \frac{\rho}{2} \cdot A \cdot c_w \cdot v^2(t) + m_{veh}\dot{v}(t)) \quad (11)$$

where m_{veh} is the mass of the vehicle, θ the road slope which is assumed to be zero, f_r the rolling friction coefficient, c_w the drag coefficient of the vehicle, ρ the density of the air, A the vehicle frontal area and v the velocity of the vehicle. The rolling friction coefficient is actually a function of the vehicle's velocity but is set to a constant value for the sake of simplicity.

3. STOCHASTIC DRIVER MODEL

In the formulation of SDP and SMPC a stochastic representation of the future driver behavior is considered. The torque required at the wheels is considered to be an disturbance input to the SMPC controller. In this paper a stationary Markov chain is used to generate driver torque demands T_{req}. Markov chains are classes of Markov processes for which state variables have finite number of values and the probability of a transition from state i in time k to state j in time $k+1$ is time invariant. As state of the Markov chain the driver torque demand at the wheels T_{req} has been considered. This variable has final number of possible states m, i.e.

$$T_{req} = \{T^1_{req}, T^2_{req}, ...T^m_{req}\} \quad (12)$$

This number is chosen in accordance with two basic requirements: to keep the computational complexity within reasonable bounds and the ability to capture the probability distribution function. Identifying the Markov chain requires transition probabilities, i.e. a transition matrix T to be estimated. This matrix is defined by the following conditional probabilities:

$$T(i,j) = Pr\{T_{req}(k+1) = T^j_{req} | T_{req}(k) = T^i_{req}\} \quad i,j = 1,...,m \quad (13)$$

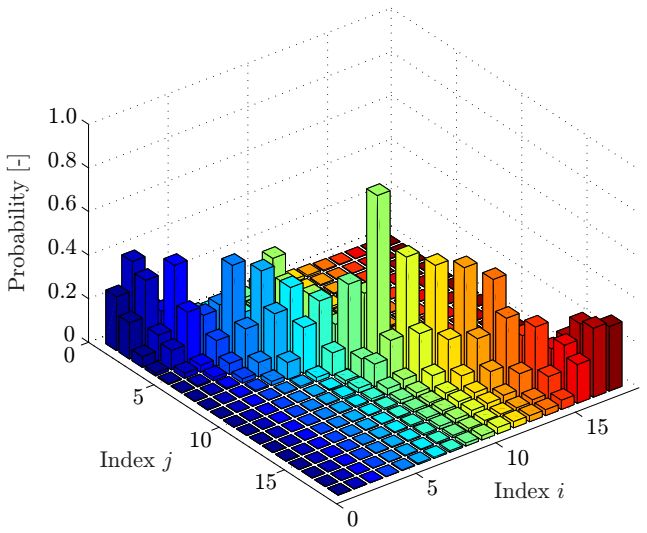

Fig. 2. Markov chain transition probability matrix with 18 states

In order to learn the transition probabilities of the Markov chain standard driving cycles (NEDC, FTP-75, FTP Highway) have been used as a training set, see Fig. 2. In simulation runs, the driver torque demand at the wheel as well as the wheel speed have been recorded. Subsequently the quantization of training data set into a final number of states has been conducted, and a smoothing technique was applied to obtain the desired transition probabilities.

In this approach we rely on a more general form of maximum likelihood estimation to represent the transition probabilities and assume that each occurrence can be assigned to more than one state in the Markov chain and the 'degree' of belonging to each state is expressed via the membership function. Let x_t be an occurrence of the requested torque in the training set. We define the membership function as in Dai [1995]:

$$m_i(x_t) = \left\{ \sum_{k=1}^{m} \left\{ \frac{d(x_t, T^i_{req})}{d(x_t, T^k_{req})} \right\}^{(F-1)} \right\}^{-1}, \quad i = 1,...,m \quad (14)$$

where $d(x_t, T^i_{req})$ denotes the Euclidean distance between measurement x_t and T^i_{req} and F is a constant that is greater than one. Using memberships for each occurrence in the training set smoothed transition probabilities are estimated to determine $T(i,j)$ in (13), i.e.

$$T(i,j) = \frac{\sum_{t=1}^{n} m_i(x_{t-1}) \cdot m_j(x_t)}{\sum_{t=2}^{n} m_i(x_{t-1})}, \quad i,j = 1,...,m \quad (15)$$

and employed in the subsequent optimization problem to predict the driver's future behavior.

4. STOCHASTIC MODEL PREDICTIVE CONTROL

We consider a state space representation of the continuous-time system with additive uncertainty w:

$$\dot{\boldsymbol{x}} = \boldsymbol{f}(\boldsymbol{x}, \boldsymbol{u}, w) \tag{16}$$

$$\boldsymbol{y} = \boldsymbol{g}(\boldsymbol{x}, \boldsymbol{u}, w) \tag{17}$$

where $\boldsymbol{x^T} = [v,\ SoC]$ denotes the state vector, $\boldsymbol{u}^T = [T_{ice},\ T_{br}]$ the control vector and $w(t)$ is an additive disturbance that represents the driver torque demand. The states of the system are the vehicle's velocity v and the battery's state of charge SoC while the control inputs are requested torque of internal combustion engine T_{ice} and the torque of the friction brakes T_{br}. In this context T_{em} is derived according to (1). The output of the system is defined as $\boldsymbol{y^T} = [\dot{m}_f,\ SoC,\ \dot{m}_{CO_2}]$ where $\dot{m}_f$ stands for the fuel mass rate, SoC for battery charge and $\dot{m}_{CO_2}$ for the rate of CO_2 emissions. In order to be applied in the predictive control scheme, (16)-(17) have to be linearized at the current operating point. Thereby the resulting discrete-time linear affine model can be represented as:

$$\boldsymbol{x}_{k+1} = \boldsymbol{A}_k\boldsymbol{x}_k + \boldsymbol{B}_k\boldsymbol{u}_k + \boldsymbol{W}_k\boldsymbol{w}_k + \boldsymbol{\Gamma}_k \tag{18}$$

$$\boldsymbol{y}_k = \boldsymbol{C}_k\boldsymbol{x}_k + \boldsymbol{D}_k\boldsymbol{u}_k + \boldsymbol{V}_k\boldsymbol{w}_k + \boldsymbol{\Delta}_k \tag{19}$$

where $\boldsymbol{A}_k \in \mathbb{R}^{2\times2}$ denotes the system matrix, $\boldsymbol{B}_k \in \mathbb{R}^{2\times2}$ the input matrix, $\boldsymbol{C}_k \in \mathbb{R}^{3\times2}$ the output matrix, $\boldsymbol{W}_k \in \mathbb{R}^3$ and $\boldsymbol{V}_k \in \mathbb{R}^3$ describe the influence of the system disturbance w on the state variables and output variables and $\boldsymbol{\Gamma}_k \in \mathbb{R}^2$ as well as $\boldsymbol{\Delta}_k \in \mathbb{R}^3$ indicate affine terms that result from the linearization at the current operating point.

In the standard MPC control formulation, starting at the current state x_k, an open-loop optimal control problem is solved over a finite prediction horizon of length H_p. Without loss of generality the quadratic cost function

$$\min_{\boldsymbol{\Delta u}}\{(\boldsymbol{y}-\boldsymbol{y}_{ref})^T\cdot\boldsymbol{Q}\cdot(\boldsymbol{y}-\boldsymbol{y}_{ref}) + \boldsymbol{\Delta u}^T\cdot\boldsymbol{R}\cdot\boldsymbol{\Delta u}\} \tag{20}$$

is minimized subjected to dynamic constraints, as well as corresponding input and state constraints. An optimal input sequence $\boldsymbol{\Delta u}^*_{(k|k)}, ..., \boldsymbol{\Delta u}^*_{(k+H_u-1|k)}$ of length H_u is obtained and only the first element is applied to the system $\boldsymbol{u}_k = \boldsymbol{u}_{k-1} + \boldsymbol{\Delta u}_{(k|k)}$. The optimization problem is repeated at time $k+1$ based on a new state measurement or estimate leading to a receding horizon control strategy.

In the stochastic MPC the system disturbance $w(t)$, i.e. the driver torque demand, is estimated along the prediction horizon using a stochastic process outlined in section 3. Unlike the standard MPC, in the SMPC the idea of multiple horizons is introduced. At each time step, based on the current value of the disturbance $w(k)$, an optimization graph is build according to Di Cairano et al. [2013]. The graph consists of nodes which represent a particular future driver request and edges that connect subsequent driver torque demands. Thereby the current torque demand is represented by the root node. In this way, the optimization tree might contain more paths, where each path represents one possible request sequence and therefore one prediction horizon. In the SMPC strategy the cost function similar to (20) is minimized considering all possible paths in the optimization graph. Starting from the root node, we propagate node wise along the graph until the leaf node of each path is reached. Compared to the standard MPC formulation, the change of the control input is assigned to each node except leaf nodes. The optimization tree generated at each time instance contains n_{max} nodes, i.e. $\mathcal{N} = \{\mathcal{N}_1, ..., \mathcal{N}_{n_{max}}\}$, where n_{max} can be set by the user in the same fashion as the prediction horizon H_p and the control horizon H_u are set in the standard MPC formulation. To each node in the graph $\mathcal{N}_i,\ i = 1, ...n_{max}$ a property set $\mathcal{P}_i$ is assigned containing the information summarized in Table 1. At each time step, the optimization tree, containing estimated future requested torque sequences, is rebuild and the SMPC optimization scheme is repeated. Compared to standard MPC, the SMPC problem exhibits slight modifications of the cost functional and is formulated as follows:

Table 1. Node content in optimization graph

Property set $\mathcal{P}_i$ of node $\mathcal{N}_i$	
$T_{req,wh,i}$	Requested wheel torque
$\omega_{req,wh,i}$	Expected wheel angular velocity
π_i	Probability of reaching node $\mathcal{N}_i$ from root node
pre_i	Index of parent (predecessor) node
$succ\_list_i$	Indices of successor nodes
$type_i$	Node indicator (node or leaf)
$T_{em,min,i}$	Minimum allowed ICE torque
$T_{em,max,i}$	Maximum allowed ICE torque
$T_{ice,min,i}$	Minimum allowed EM torque
$T_{ice,max,i}$	Maximum allowed EM torque

$$\begin{aligned}\min_{\boldsymbol{\Delta u},\epsilon_s,\epsilon_f} & \sum_{i\in\mathcal{N}\setminus\mathcal{N}_1} \pi_i\cdot(\boldsymbol{y}_i-\boldsymbol{y}_{ref})^T\cdot\boldsymbol{Q}\cdot(\boldsymbol{y}_i-\boldsymbol{y}_{ref}) \\ & + \sum_{j\in\mathcal{N}\setminus\mathcal{N}_{leaf}} \pi_j\cdot\boldsymbol{\Delta u}^T\cdot\boldsymbol{R}\cdot\boldsymbol{\Delta u} \\ & + \sum_{k\in\mathcal{N}\setminus\mathcal{N}_{leaf}} \pi_k\cdot\boldsymbol{u}^T\cdot\boldsymbol{S}\cdot\boldsymbol{u} + \alpha_s\cdot\epsilon_s + \alpha_f\cdot\epsilon_f\end{aligned} \tag{21}$$

subject to the system dynamics:

$$\boldsymbol{x}_1 = \boldsymbol{x}_k,\quad \boldsymbol{w}_1 = \boldsymbol{w}_k,\quad \boldsymbol{u}_1 = \boldsymbol{u}_k \tag{22}$$

$$\boldsymbol{x}_i = \boldsymbol{A}_k\boldsymbol{x}_{pre(i)} + \boldsymbol{B_k}\boldsymbol{u}_{pre(i)} + \boldsymbol{W}_k\omega_i + \boldsymbol{\Gamma}_k \tag{23}$$

$$\boldsymbol{y}_i = \boldsymbol{C}_k\boldsymbol{x}_{pre(i)} + \boldsymbol{D_k}\boldsymbol{u}_{pre(i)} + \boldsymbol{V}_k\omega_i + \boldsymbol{\Delta}_k,\ i\in\mathcal{N}\setminus\mathcal{N}_1 \tag{24}$$

and the following constraints:

$$T_{ice,i} \geq T_{ice,min}(\omega_{ice,i}), \qquad i = 1, ...n_{max}-1 \tag{25}$$

$$T_{ice,i} \leq T_{ice,max}(\omega_{ice,i}), \qquad i = 1, ...n_{max}-1 \tag{26}$$

$$T_{em,i} \geq T_{em,min}(\omega_{em,i}), \qquad i = 1, ...n_{max}-1 \tag{27}$$

$$T_{em,i} \leq T_{em,max}(\omega_{em,i}), \qquad i = 1, ...n_{max}-1 \tag{28}$$

$$T_{br,i} \leq 0, \qquad i = 1, ...n_{max}-1 \tag{29}$$

$$SoC_i \geq SoC_{min} - \epsilon_s, \qquad i = 1, ...n_{max}-1 \tag{30}$$

$$SoC_i \leq SoC_{max} + \epsilon_s, \qquad i = 1, ...n_{max}-1 \tag{31}$$

$$SoC_{\mathcal{N}_{leaf}} \geq SoC_{ref} - \epsilon_f,\ SoC_{\mathcal{N}_{leaf}} \leq SoC_{ref} + \epsilon_f \tag{32}$$

$$\epsilon_s \geq 0,\ \epsilon_f \geq 0 \tag{33}$$

It should be noted that integer value i refers to the index of the node in the optimization graph. The cost function of the SMPC scheme is a quadratic function and weights the deviation of control outputs $\boldsymbol{y}^T = [\dot{m}_f,\ SoC,\ \dot{m}_{C0_2}]$ from their reference values, the change of control inputs $\boldsymbol{\Delta u}^T = [\Delta T_{ice},\ \Delta T_{br}]$, the absolute values of control inputs $\boldsymbol{u}^T = [T_{ice},\ T_{br}]$ and the use of slack variables ϵ_s and ϵ_f that are employed in soft-constraints (30)-(32). The diagonal matrix $\boldsymbol{Q}$ contains scalar weights that penalize the deviation from the battery's state of charge set point SOC_{ref}, the fuel consumption $\dot{m}_{f,ref}$ and the CO_2

emission set point $\dot{m}_{CO_2,ref}$. The matrix $\boldsymbol{R}$ contains the weights for control input changes while the matrix $\boldsymbol{S}$ is used to penalize the absolute value of the control inputs. Weighting of the absolute values is used to force the control strategy to use the friction brakes only in the case when regenerative braking can not be realized. The matrices $\boldsymbol{Q}$, $\boldsymbol{R}$ and $\boldsymbol{S}$ at each node in the graph are given as: $\boldsymbol{Q} = \text{diag}(q_{\dot{m}_f}, q_{SoC}, q_{\dot{m}_{CO_2}})$, $\boldsymbol{R} = \text{diag}(r_{\Delta T_{ice}}, r_{\Delta T_{br}})$ and $\boldsymbol{S} = \text{diag}(s_{T_{ice}}, s_{T_{br}})$. It should be noted that the SMPC cost function accounts for all nodes in the optimization tree such that the optimization is performed over all possible paths in the graph.

Constraints (25)-(28) on ICE and EM torques are introduced to account for machine limitations. Thereby for each node in the scenario tree upper and lower operational limits for both propulsion machines are newly determined based on (6) and (9). The state of charge should be kept within certain operating range and the terminal constraint (32) for state of charge is introduced. This assumption is beneficial for sustaining battery charge and is commonly presented in literature, see Ambuhl and Guzzella [2009]. The main intention of employing the terminal constraint is to force the state of charge to tend towards its reference value at the end of the prediction horizon. In the SMPC scheme several prediction horizons might be available, as the graph may exhibit tree structure and contains more than one path. Therefore the terminal constraint is employed at each leaf node, as the end of a single horizon is determined by one leaf node. The battery state of charge constraint and terminal cost have been formulated as soft-constraints and the slack-variables ϵ_s and ϵ_f are used to ensure the feasibility of the optimization problem.

5. SIMULATION RESULTS

The performance of the SMPC control strategy is evaluated on the standard driving cycles NEDC, FTP-75 and FTP Highway. The obtained results are compared to a MPC controller which has a perfect knowledge of the driving cycle and therefore of the future torque demands. The simulation model employed to evaluate the performance of both strategies is a feed-forward model of a parallel HEV and all vehicle parameters and data are taken from the advanced vehicle simulator ADVISOR. The transition probability matrix T of the Markov chain, applied to predict the driving profile, is estimated offline using the training set which contains observation data from NEDC, FTP-75, FTP Highway and MODE 10-15 driving cycles. Increasing the number of states in the Markov chain leads to higher computational complexity. Thus a trade-off between the reliability of the stochastic model and computational speed is made and a Markov chain with 18 states is considered. In the smoothing technique employed for transition probability generation the parameter F is set to 1.5 as simulations have shown that taking a greater value results in strongly smoothed data set. The sampling time for both, baseline MPC and SMPC energy management strategy is chosen to be $T_s = 1s$. The following MPC parametrization has been used: $q_{\dot{m}_f} = 2$, $q_{SoC} = 2000$, $q_{\dot{m}_{CO_2}} = 0.2$, $r_{\Delta T_{ice}} = 0.01$, $r_{\Delta T_{br}} = 0$, $s_{T_{ice}} = 0$, $s_{T_{br}} = 1$ and the battery reference value is set to 60% of its charge ($SOC_{ref} = 0.6$). The weights of slack-variables ϵ_s and ϵ_f are set to 10^5 and 10^3 respectively. The optimization graph

Table 2. SMPC vs. MPC control results

Drive Cycle	CO_2 (%)	$\dot{m}_f$ (%)	Δ SoC gain/loss (%)
NEDC	+7.24	+7.1	+5.98 / +3.25
FTP-75	+0.97	+0.9	+1.30 / +0.2
FTP Highway	+2.19	+2.15	+1.03 / +2.8

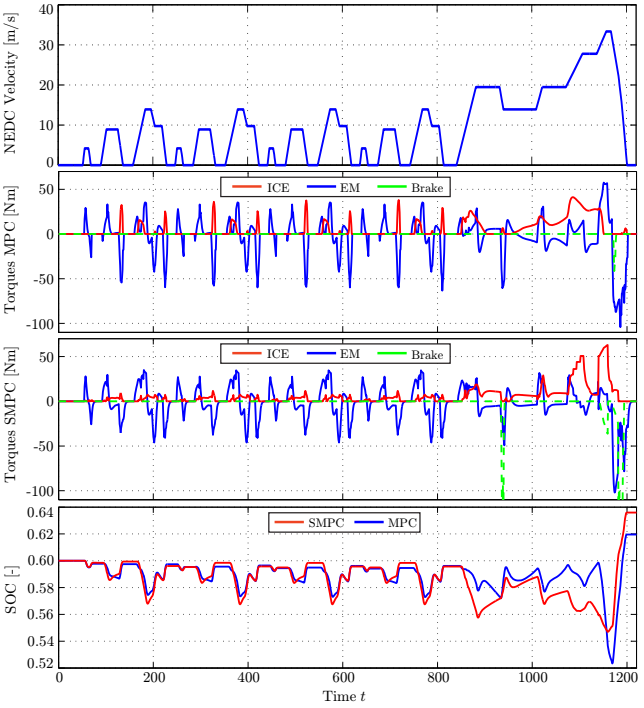

Fig. 3. Results of SMPC and MPC over NEDC cycle

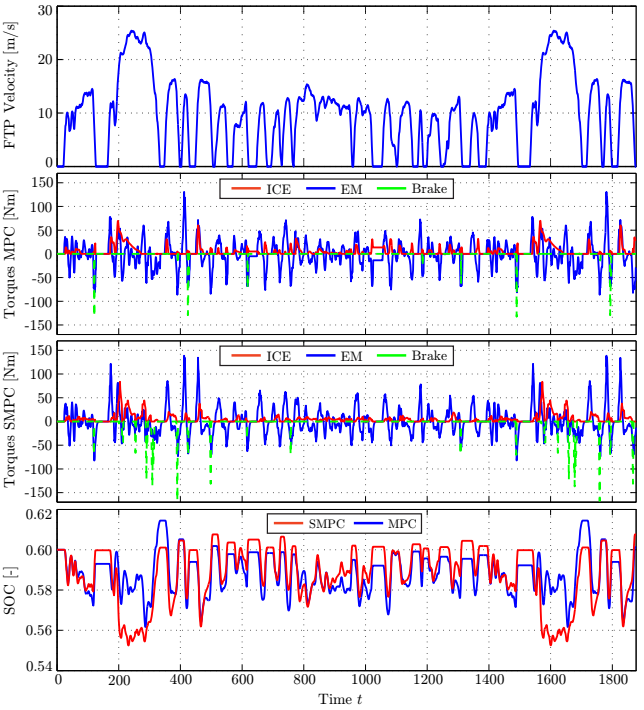

Fig. 4. Results of SMPC and MPC over FTP-75 cycle

in the SMPC scheme has 100 nodes ($n_{max} = 100$) while the prediction and control horizon in the MPC scheme used as a benchmark are $H_u = 50$ and $H_p = 50$ respectively. The

initial conditions are set to $SoC(0) = 0.6$, $T_{req} = 0\,\text{Nm}$ and $\omega_{req}(0) = 0\,\text{rad/s}$ while the lower and upper limit for SoC are selected to be $SoC_{min} = 0.5$ and $SoC_{min} = 0.7$ respectively. Furthermore, qpOASES is used as QP (active-set) solver, see Ferreau [2012].

The torque split as well as the SoC trajectories for both control strategies over the NEDC and FTP drive cycle are presented in Fig. 3 and Fig. 4 respectively. For the sake of brevity illustration of the results for FTP Highway is not shown. For most of the NEDC cycle duration the SoC trajectory of the SMPC controller lies very close to the SoC profile of the reference MPC controller. Larger deviations from the SoC of the reference controller can be noted in the range from 850 s to 1220 s for NEDC and between 200-300 s and 1580-1680 s for FTP-75 cycle and are a consequence of the uncertainties in the stochastic driver model. Table 2 contains information on how much the fuel consumption and CO_2 emissions are larger for the SMPC controller compared to reference control strategy. While the SMPC control scheme shows larger fuel consumption and CO_2 emissions of about 7% for the NEDC, these deviations are considerably small for FTP-75 and FTP Highway. From this result it can be concluded that torque demands in the NEDC are harder to predict than for the other driving cycles. Nevertheless, it can be recognized that the stochastic driver model is well suited to obtain results close to the control scheme that exploits full knowledge of the driving cycle. In addition, Table 2 provides procentual information on the deviation of the SoC from its reference value at the end of the driving cycle for both, SMPC and MPC strategy.

6. CONCLUSION AND FUTURE WORK

We have presented an energy management strategy for parallel HEVs. The aim was to optimize the fuel economy and CO_2 emission while keeping the battery's state of charge within prescribed bounds. In the realized control approach the future driving behavior has been approximated by a stochastic process. The results obtained have been compared to the MPC that has a full knowledge of a driving cycle and therefore assures good fuel economy and CO_2 emissions reduction. These indicate that SMPC is a promising control strategy for HEVs which has the advantage over deterministically based approaches that the driving cycle does not have to be known in advance and can be implemented online.

Future work will aim at integrating a prediction of future gear shifts in the SMPC scheme, defining a reference trajectory for the battery's SoC as well as the evaluation of the strategy on real driving profiles. Furthermore a comparison with other recently proposed strategies such as game theory might be a subject of further studies.

REFERENCES

D. Ambuhl and L. Guzzella. Predictive Reference Signal Generator for Hybrid Electric Vehicles. *IEEE Transactions on Vehicular Technology*, 58(9):4730–4740, 2009.

R. Beck et al. Model Predictive Control of a Parallel Hybrid Vehicle Drivetrain. In *IEEE Conference on Decision and Control and European Control Conference*, pages 2670–2675, 2005.

M. Bichi, G. Ripaccioli, S. Di Cairano, D. Bernardini, A. Bemporad, and I.V. Kolmanovsky. Stochastic model predictive control with driver behavior learning for improved powertrain control. In *IEEE Conference on Decision and Control*, pages 6077–6082, 2010.

H. Borhan, A. Vahidi, A.M. Phillips, M.L. Kuang, I.V. Kolmanovsky, and S. Di Cairano. MPC-Based Energy Management of a Power-Split Hybrid Electric Vehicle. *IEEE Transactions on Control Systems Technology*, 20 (3):593–603, 2012.

J. Dai. Isolated word recognition using markov chain models. *IEEE Transactions on Speech and Audio Processing*, 3(6):458–463, 1995.

C. Dextreit and I.V. Kolmanovsky. Game theory controller for hybrid electric vehicles. *IEEE Transactions on Control Systems Technology*, PP(99):1–1, 2013.

S. Di Cairano, D. Bernardini, A. Bemporad, and I.V. Kolmanovsky. Stochastic MPC With Learning for Driver-Predictive Vehicle Control and its Application to HEV Energy Management. *IEEE Transactions on Control Systems Technology*, PP(99):1–1, 2013.

H. J. Ferreau. qpOASES User's Manual (Version 3.0beta). *Optimization in Engineering Center (OPTEC) and Department of Electrical Engineering, KU Leuven*, 2012.

L. Guzzella and A. Sciaretta. *Vehicle Propulsion Systems*. Springer, 2013.

L. Johannesson, M. Asbogard, and B. Egardt. Assessing the potential of predictive control for hybrid vehicle powertrains using stochastic dynamic programming. In *Intelligent Transp. Systems*, pages 366–371, 2005.

J. Liu and H. Peng. Modeling and Control of a Power-Split Hybrid Vehicle. *IEEE Transactions on Control Systems Technology*, 16(6):1242–1251, 2008.

C. Musardo, G. Rizzoni, and B. Staccia. A-ECMS: An Adaptive Algorithm for Hybrid Electric Vehicle Energy Management. In *IEEE Conf. on Decision and Control and European Control Conf.*, pages 1816–1823, 2005.

D.F. Opila et al. An Energy Management Controller to Optimally Trade Off Fuel Economy and Drivability for Hybrid Vehicles. *IEEE Transactions on Control Systems Technology*, 20(6):1490–1505, 2012.

G. Ripaccioli, D. Bernardini, S. Di Cairano, A. Bemporad, and I.V. Kolmanovsky. A stochastic model predictive control approach for series hybrid electric vehicle power management. In *American Control Conference*, pages 5844–5849, 2010.

L. Serrao, S. Onori, and G. Rizzoni. ECMS as a realization of Pontryagin's minimum principle for HEV control. In *American Control Conference*, pages 3964–3969, 2009.

O. Sundstrom and L. Guzzella. A generic dynamic programming matlab function. In *IEEE Conf. on Control Appl. and Intelligent Control*, pages 1625–1630, 2009.

E.D. Tate, J.W. Grizzle, and H. Peng. Shortest path stochastic control for hybrid electric vehicles. *International Journal of Robust and Nonlinear Control*, 18: 1409–1429, 2007.

R. Wang and S.M. Lukic. Dynamic programming technique in hybrid electric vehicle optimization. In *IEEE International Electric Vehicle Conf.*, pages 1–8, 2012.

K.B. Wipke, M.R. Cuddy, and S.D. Burch. ADVISOR 2.1: a user-friendly advanced powertrain simulation using a combined backward/forward approach. *IEEE Transactions on Vehicular Technology*, 48(6):1751–1761, 1999.